

## **Interaction Notes**

**Note 628**

**June 2016**

### **EFFECTS OF DISTRIBUTED SOURCES ON TRANSMISSION-LINE MODELS: LOW FREQUENCY APPROXIMATIONS**

**J-P. Parmantier - I. Junqua - S. Bertuol - P. Schickele**

DEMR  
ONERA – The French Aerospace Lab,  
F-31055, Toulouse, France

#### **Abstract**

This paper addresses the question of integrating voltage source terms for generating equivalent distributed sources in a transmission line model. This problem is of particular interest when applying Agrawal's Field-to-Transmission-Line model in a numerical modelling procedure involving a 3D-full wave solver with a very small mesh-cell size and a MTLN solver based on the BLT resolution. It particularly stresses the importance of load conditions at the ends of the transmission-line conductors and shows that this integration is not valid for low-impedance conditions of the transmission-line. However, it shows that an equivalent source, valid for any type of load conditions on the transmission line can be defined. The demonstration is made by developing analytical solutions on a single-conductor transmission-line model loaded in 3 specific conditions: short-circuit/short-circuit, matched/matched, short-circuit/open-circuit. The paper shows that low frequency analytical solutions of BLT-based MTLN formulations are entirely compatible with equivalent electrical circuit formulations. The equation derivations are oriented in such a way to verify the conclusions on the validity of the distributed-sources integration approach. Illustrations are made with the CRIPTE code for the 3 specific load and various source-distribution conditions.

## TABLE OF CONTENTS

1.	Motivation.....	3
1.1.	MTLN theory and Field-to-Transmission-Line.....	3
1.2.	Problems observed when optimizing voltage source distribution in Agrawal’s models .....	3
1.3.	Structure of this document.....	4
2.	Presentation of the problem.....	5
2.1.	Single conductor transmission-line description.....	5
2.2.	BLT general formulation.....	6
2.3.	BLT formulation for the single conductor transmission-line model.....	7
3.	Bi directional Source Wave calculation for various cases .....	8
3.1.	General definition of $W_s$ .....	8
3.2.	Delta voltage source located at a position $d$ .....	9
3.3.	Constant voltage source located between $d_1$ and $d_2$ .....	9
3.3.1.	General expression .....	9
3.3.2.	Equivalence with a Dirac source .....	10
4.	BLT solutions of a one-conductor Transmission-line with various load and source conditions.....	10
5.	Low frequency approximation for various load and source conditions .....	13
5.1.	Low frequency derivations .....	13
5.2.	Low frequency SC/SC analysis .....	15
5.3.	Low frequency $Z_c/Z_c$ analysis.....	16
5.4.	Low frequency SC/OC analysis .....	18
6.	Influence of sources distributed on several segments .....	19
6.1.	Position of the problem .....	19
6.2.	Configuration SC/SC.....	20
6.3.	Configuration $Z_c/Z_c$ .....	20
6.4.	Configuration SC/OC .....	20
6.4.1.	General solution .....	20
6.4.2.	Application .....	21
6.5.	Equivalent source solution for low frequency approximation .....	21
6.5.1.	General solution .....	21
6.5.2.	Application .....	22
7.	Conclusion .....	25
8.	References .....	26

### Acknowledgements:

This work has been funded by the EPICEA European project under the EC H2020 Grant Agreement No 689007.

## 1. MOTIVATION

### 1.1. MTLN theory and Field-to-Transmission-Line

Multiconductor Transmission-Line-Network (MTLN) theory has proved in the past 20 years its efficiency for modelling realistic cable network architectures [1]. The BLT equation, formulated in the frequency domain, provides an efficient way to make the resolution of large wiring problems installed in 3D structures, based on EM Topology principles [2]. In such models the cable networks can be modelled as topological networks in which “tubes” represent homogeneous sections of MTLs and junctions represent connection between MTLs or end-load conditions of MTLs. Nowadays, it is a method particularly indicated to address EMC and propagation on EWIS (Electrical Wiring Interconnection System) as defined in the recent subpart H of aeronautical Certification Specification (Part 21, [3]).

Field-to-Transmission-Line (FTL) theory provides several models in order to derive the distributed voltage and current generators to be applied in MTLs models when they are submitted to EM field illuminations [4]. All those models are based on the determination of vector components of incident EM fields, that is to say EM fields in the absence of the transmission-line, taken at the location of the route of the cables. Among them, Agrawal’s model is particularly interesting for numerical modelling since only one voltage generator is required (no current generator is required). Despite several drawbacks especially due to the weakness of this field component (especially at low frequency or very close to structure walls, the Agrawal model has become the basis of a modelling procedure in which 3D solvers make the calculation of the incident fields on cable routes and the MTLN solvers make the resolution of the cable network response ([5], [6], [7]). Nowadays, such procedures are being transferred to industry with automatization of the pre-processing of the input data required for the description of the wiring topology and the description of the cable routes in 3D models.

### 1.2. Problems observed when optimizing voltage source distribution in Agrawal’s models

In Agrawal’s model, these generators are equal to the components of the incident electric field tangent to the route of the cable, which does not require any information on the local geometry of the transmission-line such as for the other models requiring transverse or normal components of the electric field (for example Taylor’s [4] or Rachidi’s models [8]).

Nevertheless, when applying Agrawal’s model, the user has to keep in mind two important requirements:

- All tangent electric fields have to be collected on the routes of the wiring, especially at the level of the ends of the wiring. This requirement is mandatory in order to respect Faraday’s law,
- This FTL model directly calculates the electrical currents but only calculates the so called “scattered voltages”<sup>1</sup>.

In the implementation of the numerical procedure with a 3D solver, the tangent electrical fields are distributed as constant values applied on intervals. As native data directly coming from the 3D calculation, the intervals are directly coming from the sampling of the mesh used for the 3D calculation. Since 3D

---

<sup>1</sup> Theoretically, the total voltage is obtained by adding the normal component of the electric field which brings back this model to the drawback mentioned for the other FTL models. However, from a practical point of view of real wiring installations, the end voltages are generally measured at the level of connectors for which the distance to the reference ground is very small and at which level the scattered voltage can be therefore approximated to the total voltage. By the way, in order to avoid any error in the determination of the voltage, the safest practice is to determine the total voltage at the ends of networks by multiplying the current by the end-impedance.

calculations are improving with capabilities of computers, meshed models become more and more precise and mesh cells smaller and smaller. The number of samples of distributed voltage sources to be transferred to MTLs models according to FTL becomes thereby very large and we may ask ourselves if such a sampling is not over-dimensioned with respect to the frequency range of interest for solving transmission-line equations. In particular, taking as a basis the generally admitted quasi static approximation based on the  $\lambda/10$  sampling required in 3D calculation, we may think of reducing this number of intervals (i.e. having cells smaller than  $\lambda/10$  is sufficient to neglect propagation in the cell and the value in the cell may be approached as constant). The number "10" is a typical value but it may vary depending on the numerical method. For those distributed generators, one reasonable idea is to integrate the generators coming from the 3D calculation on new intervals, optimized in size, as proposed in [9]. In this paper, we want to address the question of the validity of this approximation

In order to carry out this investigation, we can think of a simple model in order to simulate this phenomenon and confirm these two hypotheses. Consequently, in this paper, we consider a simple transmission-line made of only one conductor on which we apply several end-load and distributed generator configurations.

In this paper, we will call:

- "Low Frequency" (LF), the frequency regime for which the overall length of the line is much smaller than the wavelength; it is also the regime for which the transmission-line can be modelled by lumped circuit elements. It refers to frequencies before the first resonance of the line.
- "High Frequency" (HF), the frequency regime for which the overall length becomes in the same order of magnitude as the wavelength or larger than the wavelength; it is the regime for which the transmission-line modelling requires taking into account its propagation characteristics (propagation matrix, characteristic impedance). It refers to all frequencies when the line resonates.

The application in this paper is made with a 2m-long transmission line with various load conditions. Therefore, the first smallest resonance frequency is when the length of the line is equal to  $\lambda/4$  ( $\lambda$ =wavelength), i.e. 35 MHz. In order to be outside of the variation of this first smallest resonance frequency, the limit of the LF regime must be taken under this resonance frequency. This is why the LF frequency limit is chosen at 10 MHz in our example.

### **1.3. Structure of this document**

Section 2 introduces the one-conductor transmission-line model as well as the BLT general solution that will be used in the following sections. This section also introduces a generic example of a transmission-line made of a wire over a ground plane that will be used in the illustrations of the results.

Section 3 presents several analytical solutions of source-waves to be used in the general solution developed in section 2, for various configurations of constant per-unit-length (p.u.l.) voltage source. Since the motivation of this paper is to investigate Agrawal's numerical implementation, only distributed voltage sources will be considered in this paper.

Section 4 introduces several load conditions of the transmission-line and summarizes the wideband BLT solution, for the various source wave configurations presented in section 2. We consider two extreme end-conditions: a short-circuit/short-circuit configuration and a short-circuit/open circuit configuration. In addition, we also consider a matched/matched configuration as a transition between the two extreme conditions.

Section 5 takes the results of section 4 and studies the low frequency variations of currents and voltages at both ends of the transmission-line. The question of the independence of the response as a function of the position of the source is asked.

Section 6 takes the results of section 5 and considers the effect of distributing p.u.l. sources of various constant values on intervals and asks the question of simplifying this distribution at low frequency by integrating them. It finally addresses the question of a possible equivalent source model for low frequency approximation valid for any load configuration and any source.

Finally, section 7 concludes on the rules for integrating voltage sources on a transmission-line in order to lower the number of voltage generators.

The reference validations displayed in this paper are made numerically with the CRIPTE code [10]. This software has been validated among many applications in the past 20 years.

## 2. PRESENTATION OF THE PROBLEM

### 2.1. Single conductor transmission-line description

In this paper, we consider a single conductor transmission-line connecting two end-impedances  $Z_1$  and  $Z_2$ . Its length is  $\ell$ . The transmission-line will represent any type of geometry (two wires, wire over a ground plane, coaxial, shielded). On this transmission-line, we define two opposite directions of propagation  $z_1$  and  $z_2$ . According to these two directions of propagation, we define voltage and current quantities  $V_1(z_1)$  and  $I_1(z_1)$  on the one hand and  $V_2(z_2)$  and  $I_2(z_2)$  on the other hand. At each end, those quantities take the value  $V_1(0)$ ,  $I_1(0)$ ,  $V_2(\ell)$  and  $I_2(\ell)$ , at the origin and the remote extremities according to  $z_1$  and  $z_2$  respectively. On this tube we consider also a distribution of p.u.l. voltage sources  $V_s(z)$  that will be written  $V_{s1}(z_1)$  and  $V_{s2}(z_2)$  according to  $z_1$  and  $z_2$  directions of propagation.

At a given position  $z_2 = \ell - z_1$ , we can write:

$$\begin{aligned} V_{s1}(z_1) &= -V_{s2}(z_2) = -V_{s2}(\ell - z_1) \\ I_1(z_1) &= -I_2(z_2) \\ V_1(z_1) &= V_2(z_2) \end{aligned} \tag{1}$$

Since in this paper the transmission-line problem is supposed to simulate voltage sources coming from Agrawal's model, note that  $V_1(z)$  and  $V_2(z)$  must be understood as scattered voltages as mentioned in paragraph 1.2. As specified in the introduction, we do not consider any current sources.

In Figure 1, we consider as an illustration a transmission-line made of a wire in free space over an infinite perfectly conducting ground plane (height of wire = 10 cm, radius of wire = 1 mm). The following values will be taken for the numerical and mathematical applications:

- Per-unit-length inductance:  $L = 0.6 \mu\text{H/m}$
- Per-unit-length capacitance:  $C = 18.5 \text{ pF/m}$  (transmission-line in free space)
- Per-unit-length resistance:  $R = 1.1 \text{ m}\Omega/\text{m}$
- Per-unit-length conductance:  $G = 0 \text{ S/m}$
- Length :  $\ell = 2 \text{ m}$

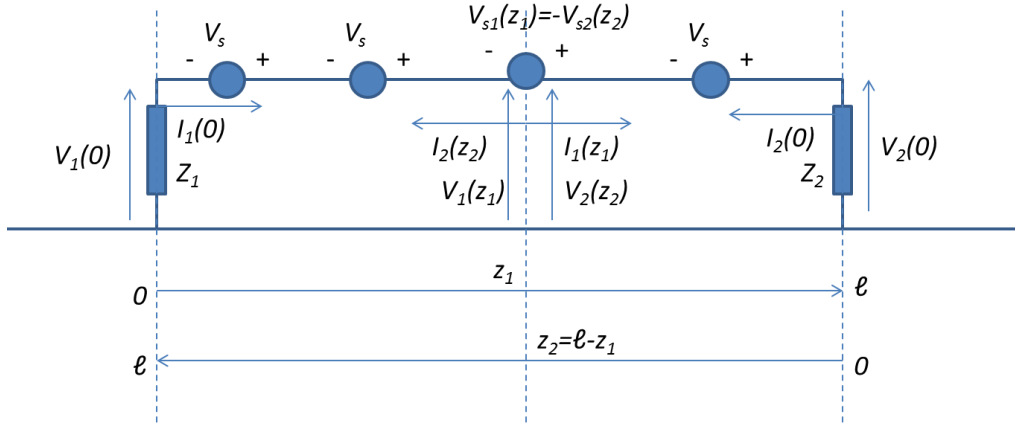


Figure 1 : One wire transmission-line example used for validations

From the above values we can determine:

$$Z_c = \sqrt{\frac{(R + jL\omega)}{jC\omega}} \quad (2)$$

the characteristic impedance and its usual approximation at high frequency  $Z_c = \sqrt{\frac{L}{C}} = 180 \Omega$

$$v = \frac{1}{\sqrt{LC}} \quad (3)$$

the propagation velocity and its value  $v = 3.10^8$  m/s, as expected in free space

$$\gamma(\omega) = \sqrt{j\omega C \cdot (R + jL\omega)} \quad (4)$$

the propagation coefficient of the transmission-line with its usual high frequency approximation:

$$\gamma(\omega) = \sqrt{j\omega C \cdot (R + jL\omega)} \xrightarrow{L\omega \gg R} \gamma(\omega) = \omega\sqrt{LC} = \frac{\omega}{v} \quad (5)$$

Note that for the validations, we chose to have only resistance losses and no conductance losses ( $G=0$ ), which covers a large number of situations of transmission-lines. We'll see later on in this paper that the interest of this approximation is that we have  $\gamma \xrightarrow{\omega \rightarrow 0} 0$ .

## 2.2. BLT general formulation

The wave formulation of the BLT equation as defined by C.E. Baum [1] can be written as follows:

$$([Id] - [S][\Gamma])[W(0)] = [S][W_s] \quad (6)$$

where:

- $[I/d]$  represents the unit matrix,
- $[S]$  the network supermatrix, made of the S-parameters of the junctions organized in matrix blocks with respect to the topology of the network,
- $[\Gamma]$  the network propagation supermatrix made of the propagation matrices of the tubes,
- $[W(0)]$  the outgoing waves supervector of the network,
- $[W_s]$  the source-wave supervector.

### 2.3. BLT formulation for the single conductor transmission-line model

Figure 2 represents the topological network of the one-conductor transmission-line described in Figure 1. It is made of a single tube connected to two junctions  $J_1$  and  $J_2$ , representing the two end-impedances  $Z_1$  and  $Z_2$ .  $W_1(z_1)$  is the wave propagating along the  $z_1$  direction and  $W_2(z_2)$  is the wave propagating along the  $z_2$  direction.  $W_1(0)$  and  $W_2(0)$  on the one hand, and  $W_1(\ell)$  and  $W_2(\ell)$  on the other hand are the waves at the origin and the end of the directions of propagation  $z_1$  and  $z_2$  respectively.  $W_{s1}$  and  $W_{s2}$  represent the source waves according to  $z_1$  and  $z_2$  derived from the collections of the various p.u.l. voltage generators  $V_{s1}(z_1)$  (and  $V_{s2}(z_2)$ ), according to  $z_1$  (and  $z_2$ ).

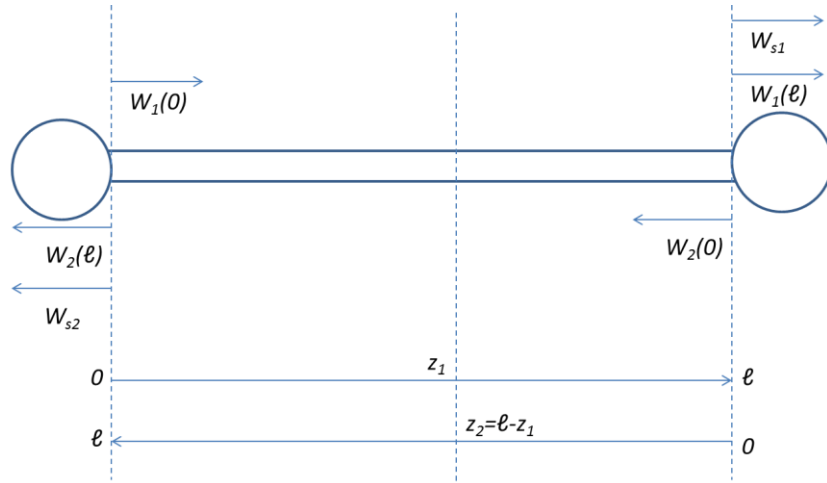


Figure 2 : Topological network and propagation waves for a one-tube topological network

We call:

- $\Gamma$  the propagation matrix of the tube with  $\Gamma = e^{-\gamma \ell}$ , with  $\gamma$  the propagation coefficient of the tube.
- $S_1$  and  $S_2$  the two S-parameters of junctions  $J_1$  and  $J_2$ .

The BLT equation of this particular network can be derived in the following matrix form:

$$\left( \begin{bmatrix} 1 & 0 \\ 0 & 1 \end{bmatrix} - \begin{bmatrix} 0 & S_1 \\ S_2 & 0 \end{bmatrix} \cdot \begin{bmatrix} \Gamma & 0 \\ 0 & \Gamma \end{bmatrix} \right) \cdot \begin{pmatrix} W_1(0) \\ W_2(0) \end{pmatrix} = \begin{bmatrix} 0 & S_1 \\ S_2 & 0 \end{bmatrix} \cdot \begin{pmatrix} W_{s1} \\ W_{s2} \end{pmatrix} \quad (7)$$

Equation (7) leads to the general solutions of  $W_1(0)$  and  $W_2(0)$ :

$$\begin{cases} W_1(0) - S_1 \cdot \Gamma \cdot W_2(0) = S_1 \cdot W_{s2} \\ -S_2 \cdot \Gamma \cdot W_1(0) + W_2(0) = S_2 \cdot W_{s1} \end{cases} \quad (8)$$

From the resolution of this system of two equations providing the two unknowns  $W_1(0)$  and  $W_2(0)$  solutions, we can derive the expressions of  $W_1(\ell)$  and  $W_2(\ell)$  from either the two propagation equations:

$$\begin{aligned} W_1(\ell) &= \Gamma.W_1(0) + W_{s1} \\ W_2(\ell) &= \Gamma.W_2(0) + W_{s2} \end{aligned} \quad (9)$$

or the two scattering equations at junctions  $J_1$  and  $J_2$ .

$$\begin{aligned} W_1(\ell) &= S_2^{-1}.W_2(0) \\ W_2(\ell) &= S_1^{-1}.W_1(0) \end{aligned} \quad (10)$$

From the solution of the waves obtained in section 2 and the various source-wave solutions derived in section 3, we can derive the explicit solutions of end-voltages and currents for various end-load and voltage source distribution conditions.

Classically, the combination of  $W_1(0)$ ,  $W_2(0)$ ,  $W_1(\ell)$  and  $W_2(\ell)$  solutions in equations (8), (9) and (10) allows the derivations of voltages and currents at each extremity of the transmission-line,  $V_1(0)$ ,  $V_2(0)$ ,  $V_1(\ell)$  and  $V_2(\ell)$ . We have:

$$V_1(0) = \frac{W_1(0) + W_2(\ell)}{2} \quad (11)$$

$$V_2(0) = \frac{W_2(0) + W_1(\ell)}{2} \quad (12)$$

$$I_1(0) = \frac{W_1(0) - W_2(\ell)}{2Z_c} \quad (13)$$

$$I_2(0) = \frac{W_2(0) - W_1(\ell)}{2Z_c} \quad (14)$$

where  $Z_c$  represents the characteristic impedance of the transmission-line.

Since the general explicit expression of  $V_1(0)$ ,  $V_2(0)$ ,  $V_1(\ell)$  and  $V_2(\ell)$  is quite complex, we calculated them by deriving specifically  $W_1(0)$ ,  $W_2(0)$ ,  $W_1(\ell)$  and  $W_2(\ell)$  for each specific configuration of end-loads.

### 3. BI DIRECTIONAL SOURCE WAVE CALCULATION FOR VARIOUS CASES

#### 3.1. General definition of $W_s$

$$W_{s1} = \int_0^{\ell} e^{-\gamma(\ell-z_1)} V_{s1}(z_1) dz_1 \quad (15)$$

$$W_{s2} = \int_0^{\ell} e^{-\gamma(\ell-z_2)} V_{s2}(z_2) dz_2$$

Where  $V_{s1}(z_1)$  and  $V_{s2}(z_2)$  represent the p.u.l. values of the distributed voltage sources  $V_s(z)$  according the directions of propagation  $z_1$  and  $z_2$ . Note that  $W_{s1}$  and  $W_{s2}$  have dimensions of volts as well.

### 3.2. Delta voltage source located at a position $d$

We consider a Dirac (“delta”) source of amplitude  $V_0$  located at a position “ $d$ ”, between 0 and  $\ell$ .

In the sense of the theory of distributions, we have:

$$\begin{aligned} V_{s1}(z_1) &= V_0 \delta(d - z_1) \\ V_{s2}(z_2) &= -V_{s1}(\ell - z_2) = -V_0 \delta(\ell - d - z_2) \end{aligned} \quad (16)$$

Equations (15) give:

$$\begin{aligned} W_{s1} &= \int_0^{\ell} e^{-\gamma(\ell-z_1)} V_0 \delta(d - z_1) dz_1 = \Gamma e^{-\gamma d} V_0 \\ W_{s2} &= -\Gamma \int_0^{\ell} e^{-\gamma z_2} V_0 \delta(\ell - d - z_2) dz_2 = -e^{-\gamma d} V_0 \end{aligned} \quad (17)$$

In particular, when  $d = 0$ , the source is localized at the origin of the transmission-line ( $J_1$ ) and we have:

$$\begin{aligned} W_{s1} &= \Gamma V_0 \\ W_{s2} &= -V_0 \end{aligned} \quad (18)$$

When  $d = \ell$ , the source is localized at the remote end of the transmission-line ( $J_2$ ) and we have:

$$\begin{aligned} W_{s1} &= V_0 \\ W_{s2} &= -\Gamma V_0 \end{aligned} \quad (19)$$

### 3.3. Constant voltage source located between $d_1$ and $d_2$

#### 3.3.1. General expression

Now we consider a distribution of constant per-unit-length (p.u.l.) generators  $V_s(z_1)$  (i.e.  $V_s(z_2)$ ) as well) distributed between the position  $d_1$  and the position  $d_2$ , with  $d_2 > d_1$  and with a total voltage equal to  $V_0$ .

$$V_{s1}(z_1) = V_{s2}(z_2) = \frac{V_0}{2 \cdot \Delta \ell_i} \quad (20)$$

Both  $d_1$  and  $d_2$  are between 0 and  $\ell$ . For this, we consider an interval such that:

$$\begin{aligned} d_2 - d_1 &= 2 \cdot \Delta \ell_i, \text{ and a medium position} \\ \ell_i &= d_1 + \Delta \ell_i = (d_1 + d_2) / 2 \end{aligned} \quad (21)$$

Then  $d_1$  and  $d_2$  take the following values:

$$\begin{aligned} d_1 &= \ell_i - \Delta \ell_i, \text{ and} \\ d_2 &= \ell_i + \Delta \ell_i \end{aligned} \quad (22)$$

Equations (15) become:

$$\begin{aligned}
W_{s1} &= \int_{\ell_i - \Delta\ell_i}^{\ell_i + \Delta\ell_i} \frac{V_{s1}(z_1)}{2\Delta\ell_i} e^{-\gamma(\ell - z_1)} dz_1 = \frac{\Gamma V_0}{2\gamma\Delta\ell_i} e^{\gamma\ell_i} (e^{\gamma\Delta\ell_i} - e^{-\gamma\Delta\ell_i}) = \frac{\Gamma V_0}{\gamma\Delta\ell_i} e^{\gamma\ell_i} \sinh(\gamma\Delta\ell_i) \\
W_{s2} &= \int_{\ell - \ell_i + \Delta\ell_i}^{\ell - \ell_i - \Delta\ell_i} \frac{V_{s2}(z_2)}{2\Delta\ell_i} e^{-\gamma(\ell - z_2)} dz_2 = -\frac{V_0}{2\gamma\Delta\ell_i} e^{-\gamma\ell_i} (e^{\gamma\Delta\ell_i} - e^{-\gamma\Delta\ell_i}) = -\frac{V_0}{\gamma\Delta\ell_i} e^{-\gamma\ell_i} \sinh(\gamma\Delta\ell_i)
\end{aligned} \tag{23}$$

### 3.3.2. Equivalence with a Dirac source

We consider a Dirac source of amplitude  $V_{sd}$ , positioned in  $d = \ell_i = (d_1 + d_2)/2$ . Equations (17) become  $W_{s1}^\delta$  and  $W_{s2}^\delta$  and are written as:

$$\begin{aligned}
W_{s1}^\delta &= \int_0^\ell V_{sd} e^{-\gamma(\ell - z_1)} \delta(z_1 - \ell_i) dz_1 = \Gamma V_{sd} e^{\gamma\ell_i} \\
W_{s2}^\delta &= -\int_0^\ell V_{sd} e^{-\gamma(\ell - z_2)} \delta(\ell - \ell_i - z_2) dz_2 = -V_{sd} e^{-\gamma\ell_i}
\end{aligned} \tag{24}$$

Comparing equations (23) and (24), we see that a total voltage source distributed between  $d_1 = \ell_i - \Delta\ell_i$  and  $d_2 = \ell_i + \Delta\ell_i$  is equivalent to a Dirac source located in  $\ell_i$  and having an amplitude:

$$V_{sd} = \frac{V_0}{2\gamma\Delta\ell_i} (e^{\gamma\Delta\ell_i} - e^{-\gamma\Delta\ell_i}) = \frac{V_0}{\gamma\Delta\ell_i} \sinh(\gamma\Delta\ell_i) \tag{25}$$

As verification, from equations (23), we consider  $\Delta\ell_i = \ell/2$  and  $\ell_i = \ell/2$ , we find the expression of the source wave when a total voltage source  $V_0$  is distributed all along  $\ell$ :

$$\begin{aligned}
W_{s1} &= \frac{V_0}{\gamma\ell} (1 - \Gamma) \\
W_{s2} &= -\frac{V_0}{\gamma\ell} (1 - \Gamma) = -W_{s1}
\end{aligned} \tag{26}$$

And, from equation (25), the amplitude of the equivalent Dirac source located at  $d = \ell/2$  is equal to:

$$V_{sd} = \frac{V_0}{\gamma\ell} (e^{\gamma\frac{\ell}{2}} - e^{-\gamma\frac{\ell}{2}}) = \frac{V_0}{\gamma\ell\sqrt{\Gamma}} (1 - \Gamma) \tag{27}$$

## 4. BLT SOLUTIONS OF A ONE-CONDUCTOR TRANSMISSION-LINE WITH VARIOUS LOAD AND SOURCE CONDITIONS

In this section, we consider various conditions of distributed p.u.l. voltage  $V_{s1}(z)$  sources distributed between  $z_1 = d_1$  and  $z_1 = d_2$ . Those two positions are defined as in (22) as a function of a center position  $\ell_i$  between  $z_1$  and  $z_2$ , the length of the distribution section been given by  $2\Delta\ell_i$  as in (21).

We also suppose that the total source integrated on the whole source distribution section is equal to  $V_0$ . We can therefore write:

$$\int_{d_1}^{d_2} V_{s1}(z_1) dz_1 = V_0 \tag{28}$$

Table 1 summarizes the results obtained on the 3 load configurations addressed in this paper:

- **SC/SC** ( $S_1 = S_2 = -1$ ) for which we have a short circuit both on  $J_1$  and  $J_2$ . This configuration is the one for which the current is maximum at both ends. The resolution of the BLT equation directly gives  $V_1(0) = V_2(0) = 0$
- **SC/OC** ( $S_1 = -1$  and  $S_2 = +1$ ) for which we have a short-circuit on  $J_1$  and an open circuit on  $J_2$ . This configuration is the one for which the  $I_1(0)$  current is minimum on  $J_1$ . The resolution of the BLT equation directly gives  $V_1(0) = 0$  and  $I_2(0) = 0$
- **Zc/Zc** ( $S_1 = S_2 = 0$ ) is a medium configuration in the middle of the two previous extreme SC/SC and SC/OC configurations, for which we have matched conditions at both on  $J_1$  and  $J_2$ . The resolution of the BLT equation directly gives  $W_1(0) = 0$  and  $W_2(0) = 0$

The p.u.l. source distribution configurations addressed are:

- **Source config. 1:** Distributed between  $z_1 = d_1$  and  $z_1 = d_2$  (general formula)
- **Source config. 2:** Dirac source localized at the origin of the transmission-line. So we have:  $\Delta\ell_i \rightarrow 0$  and  $\ell_i = 0$
- **Source config. 3:** Dirac source localized in the middle of the transmission-line. So we have:  $\Delta\ell_i \rightarrow 0$  and  $\ell_i = \ell/2$
- **Source config. 4:** Distributed on the whole length  $\ell$  of the transmission-line. So we have:  $d_1 = 0$  and  $d_2 = \ell$  (general formula)

Derivation of the solutions can take advantage of the equivalent source model defined in (27). For Dirac source configurations (Source config. 1 and Source config. 2), we make  $\Delta\ell_i \rightarrow 0$ . We note that the result does not depend on  $\ell_i$  and we have:

$$V_{sd} = \frac{V_0}{\gamma\Delta\ell_i} \sinh(\gamma\Delta\ell_i) \xrightarrow{\Delta\ell_i \rightarrow 0} V_0 \quad (29)$$

In Table 1 we can make the observations that for sources distributed on the whole length of the transmission-line, we find exactly the same solution, except a different sign for the SC/SC and Zc/Zc load configurations, due to the symmetry of the problem.

**Table 1 : End voltages and currents for various source and load configurations of the transmission-line**

	<b>Source config. 1</b> $V_{s1}(z_1) = \frac{V_0}{d_2 - d_1}$		<b>Source config. 2</b> $V_{s1}(z_1) = V_0 \delta(z_1)$		<b>Source config. 3</b> $V_{s1}(z_1) = V_0 \delta(z_1 - \frac{\ell}{2})$		<b>Source config. 4</b> $V_{s1}(z_1) = \frac{V_0}{\ell}$	
<b>SC/SC</b>	$I_1(0) = \frac{V_0}{\gamma \Delta \ell_i Z_c (1 - \Gamma^2)} \sinh(\gamma \Delta \ell_i) (\Gamma^2 e^{\gamma \ell_i} + e^{-\gamma \ell_i})$	(30)	$I_1(0) = \frac{V_0}{Z_c} \frac{1 + \Gamma^2}{1 - \Gamma^2}$	(31)	$I_1(0) = \frac{V_0}{Z_c} \frac{\sqrt{\Gamma}}{1 - \Gamma}$	(32)	$I_1(0) = \frac{V_0}{Z \ell}$	(33)
	$I_2(0) = -\frac{V_0}{\gamma \Delta \ell_i Z_c (1 - \Gamma^2)} \sinh(\gamma \Delta \ell_i) \Gamma (e^{\gamma \ell_i} + e^{-\gamma \ell_i})$		$I_2(0) = -\frac{V_0}{Z_c} \frac{2\Gamma}{1 - \Gamma^2}$		$I_2(0) = -\frac{V_0}{Z_c} \frac{\sqrt{\Gamma}}{1 - \Gamma}$		$I_2(0) = -\frac{V_0}{Z \ell} = -I_1(0)$	
<b>Z<sub>c</sub>/Z<sub>c</sub></b>	$V_1(0) = -\frac{V_0}{2\gamma \Delta \ell_i} e^{-\gamma \ell_i} \sinh(\gamma \Delta \ell_i)$	(34)	$V_1(0) = -\frac{V_0}{2}$	(35)	$V_1(0) = \frac{V_0 \sqrt{\Gamma}}{2}$	(36)	$V_1(0) = -\frac{V_0}{\gamma \ell} e^{\frac{\gamma \ell}{2}} \sinh\left(\frac{\gamma \ell}{2}\right)$	(37)
	$V_2(0) = \frac{\Gamma V_0}{2\gamma \Delta \ell_i} e^{\gamma \ell_i} \sinh(\gamma \Delta \ell_i)$		$V_2(0) = \frac{V_0}{2} \Gamma$		$V_2(0) = -\frac{V_0 \sqrt{\Gamma}}{2}$		$V_2(0) = \frac{V_0}{\gamma \ell} e^{\frac{\gamma \ell}{2}} \sinh\left(\frac{\gamma \ell}{2}\right)$	
	$I_1(0) = \frac{V_0}{2\gamma Z_c \Delta \ell_i} e^{-\gamma \ell_i} \sinh(\gamma \Delta \ell_i)$	(38)	$I_1(0) = -\frac{V_0}{2Z_c}$	(39)	$I_1(0) = -\frac{V_0 \sqrt{\Gamma}}{2Z_c}$	(40)	$I_1(0) = \frac{V_0}{Z \ell} e^{\frac{\gamma \ell}{2}} \sinh\left(\frac{\gamma \ell}{2}\right)$	(41)
	$I_2(0) = -\frac{\Gamma V_0}{2\gamma Z_c \Delta \ell_i} e^{\gamma \ell_i} \sinh(\gamma \Delta \ell_i)$		$I_2(0) = \frac{V_0}{2Z_c} \Gamma$		$I_2(0) = \frac{V_0 \sqrt{\Gamma}}{2Z_c}$		$I_2(0) = -\frac{V_0}{Z \ell} e^{\frac{\gamma \ell}{2}} \sinh\left(\frac{\gamma \ell}{2}\right)$	
<b>SC/OC</b>	$V_2(0) = \frac{V_0 \sinh(\gamma \Delta \ell_i)}{\gamma \Delta \ell_i} \cdot \frac{\Gamma (e^{\gamma \ell_i} + e^{-\gamma \ell_i})}{1 + \Gamma^2}$	(42)	$V_2(0) = \frac{2\Gamma V_0}{1 + \Gamma^2}$	(43)	$V_2(0) = \frac{V_0 \sqrt{\Gamma} (1 + \Gamma)}{1 + \Gamma^2}$	(44)	$V_2(0) = \frac{V_0}{\gamma \ell} \frac{1 - \Gamma^2}{1 + \Gamma^2}$	(45)
	$I_1(0) = \frac{V_0 \sinh(\gamma \Delta \ell_i)}{\gamma \Delta \ell_i} \cdot \frac{(e^{-\gamma \ell_i} - \Gamma^2 e^{\gamma \ell_i})}{Z_c (1 + \Gamma^2)}$		$I_1(0) = \frac{V_0 (1 - \Gamma^2)}{Z_c (1 + \Gamma^2)}$		$I_1(0) = \frac{V_0 \sqrt{\Gamma} (1 - \Gamma)}{Z_c (1 + \Gamma^2)}$		$I_1(0) = \frac{V_0}{\gamma Z_c \ell} \frac{(1 - \Gamma)^2}{(1 + \Gamma^2)}$	

## 5. LOW FREQUENCY APPROXIMATION FOR VARIOUS LOAD AND SOURCE CONDITIONS

### 5.1. Low frequency derivations

In the following section, we'll take the results of Table 1 and make the approximation  $\omega \rightarrow 0$ , with  $\omega = 2\pi f$ ,  $f$  being the frequency. When  $\omega \rightarrow 0$ ,  $\gamma(\omega)$  in (4) can be approximated as:

$$\gamma(\omega) = \sqrt{j\omega C(R + jL\omega)} \xrightarrow{\omega \rightarrow 0} 0 \quad (46)$$

and:

$$e^{\pm\gamma \cdot z} \xrightarrow{\omega \rightarrow 0} 1 \pm \gamma z \quad (47)$$

Using the low frequency approximation of the exponential in (27), we have:

$$V_{sd} = \frac{V_0}{2\gamma\Delta\ell_i} (e^{\gamma\Delta\ell_i} - e^{-\gamma\Delta\ell_i}) \xrightarrow{\omega \rightarrow 0} V_0 \quad (48)$$

We note also the following relations:

$$Z_c \gamma \ell = (R + j\omega L)\ell \quad (49)$$

$$\frac{\gamma}{Z_c} = jC\omega \quad (50)$$

(remember that our models supposes that  $G = 0$ , see paragraph 2.1).

**Table 2** presents the various low frequency approximation results derived from Table 1.

**Table 2: Low frequency approximation of end voltages and currents for various source and load configurations of the transmission-line**

	<b>Source config. 1</b> $V_{s1}(z_1) = \frac{V_0}{d_2 - d_1}$		<b>Source config. 2</b> $V_{s1}(z_1) = V_0 \delta(z_1)$		<b>Source config. 3</b> $V_{s1}(z_1) = V_0 \delta(z_1 - \frac{\ell}{2})$		<b>Source config. 4</b> $V_{s1}(z_1) = \frac{V_0}{\ell}$	
<b>SC/SC</b>	$I_1(0) \xrightarrow{\omega \rightarrow 0} \frac{V_0}{Z\ell}$	(51)	Idem (51)		Idem (51)		Idem (51)	
	$I_2(0) \xrightarrow{\omega \rightarrow 0} -\frac{V_0}{Z\ell}$							
<b>Z<sub>c</sub>/Z<sub>c</sub></b>	$V_1(0) \xrightarrow{\omega \rightarrow 0} -\frac{V_0}{2}$	(52)	Idem (52)		Idem (52)		Idem (52)	
	$V_2(0) \xrightarrow{\omega \rightarrow 0} \frac{V_0}{2}$							
	$I_1(0) \xrightarrow{\omega \rightarrow 0} \frac{V_0}{2Z_c}$	(53)	Idem (53)		Idem (53)		Idem (53)	
	$I_2(0) \xrightarrow{\omega \rightarrow 0} -\frac{V_0}{2Z_c}$							
<b>SC/OC</b>	$V_2(0) \xrightarrow{\omega \rightarrow 0} V_0$	(54)	Idem (54)		Idem (54)		Idem (54)	
	$I_1(0) \xrightarrow{\omega \rightarrow 0} jC\omega(\ell - \ell_i)V_0$	(55)	$I_1(0) \xrightarrow{\omega \rightarrow 0} jC\omega\ell V_0$	(56)	$I_1(0) \xrightarrow{\omega \rightarrow 0} \frac{jC\ell\omega}{2} V_0$	(57)	$I_1(0) \xrightarrow{\omega \rightarrow 0} \frac{jC\ell\omega}{2} V_0$	(58)

## 5.2. Low frequency SC/SC analysis

In SC/SC configuration, the low frequency expressions of  $I_1(0)$  and  $I_2(0)$  do not depend on the positions  $d_1$  and  $d_2$  (51). The expression obtained is equal to the resolution of an electrical circuit model, equivalent at low frequency, in which the impedance of the loop is made by the total impedance of the transmission-line only,  $Z = (R + j\omega)\ell$ , since the end loads are short-circuits (Figure 3).

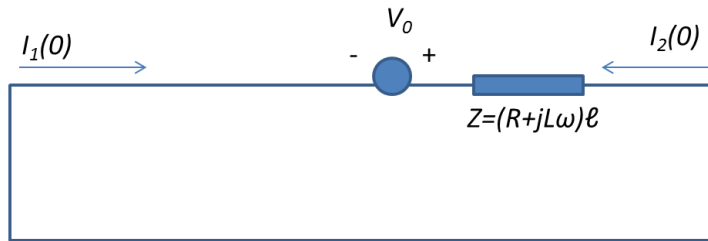


Figure 3 : Equivalent electrical circuit at low frequency for the SC/SC configuration

Figure 4 shows a comparison of the result of the currents at  $J_1$  and  $J_2$  for the one-conductor transmission-line presented in Figure 1 in the following source configurations:

- CRIPTE calculation for a Dirac source  $V_0 = 1V$  localized at the beginning of the transmission-line (legend “Loc Source Left”),
- CRIPTE calculation for a Dirac source  $V_0 = 1V$  localized in the middle of the transmission-line (legend “Loc Source Middle”),
- CRIPTE calculation for a total source  $V_0 = 1V$  distributed along  $\ell$  (legend “Dist Source”),
- Analytical calculation for the low frequency approximation of the 3 previously mentioned source configurations, (legend “BF approx.”).

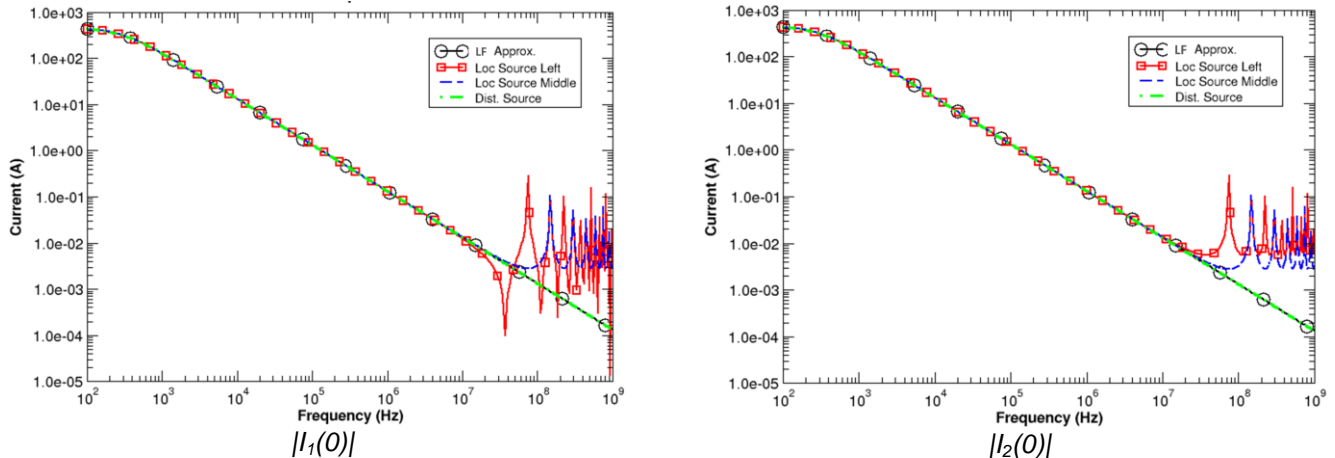


Figure 4 : Comparisons of magnitudes of currents  $I_1(0)$  (left) and  $I_2(0)$  (right) obtained in SC/SC configuration ( $V_0=1V$ )

The following observations can be made:

- In the configuration of the Dirac source excitation at the level of  $J_1$ , the currents present typical responses of near-end response (with zeros between resonances) and far-end response (with

minima between resonances) signal observed on transmission-lines excited at one extremity (equations (31)).

- In the configuration of the Dirac source excitation in the middle of the transmission-line, we confirm that currents at both extremities are similar (equations (32)). We also verify that responses for local excitation at the beginning and in the middle have respectively resonances in  $\lambda/2$  and  $\lambda$ .
- In the distributed source configuration, we confirm that the currents at each extremity are equal in module and do not present any resonance (equations (33)). The cutoff frequency is equal to  $f_c = \frac{R}{2\pi L}$   $f_c = \frac{R}{2\pi L} = 292$  Hz (with the p.u.l. parameters defined in 2.1, and corresponds to the cutoff frequency of the equivalent circuit. At low frequency, the plateau corresponds to the resistance regime and  $I_1(0) = \frac{V_0}{R \cdot \ell}$ . Over  $f_c$ , the current varies as  $I_1(0) = \frac{V_0}{j\omega L \cdot \ell}$  and is dominated by the inductance.
- Finally, at low frequency (before resonance regime, i.e. under about 10 MHz), the four plots are superposed which demonstrates that at low frequency, the result does not depend on the position of the source (equations (51)).

### 5.3. Low frequency $Z_c/Z_c$ analysis

Accounting for (30) to (33), we can show that both types of solutions for localized and distributed generators lead to the same approximations at low frequency.

In terms of equivalent electrical circuit, the results are equivalent to solve the electrical circuit model of the line loop loaded by two  $Z_c$  loads and excited by a series voltage generator  $V_0$ . The voltage obtained on each load is equal in amplitude and opposite (Figure 5).

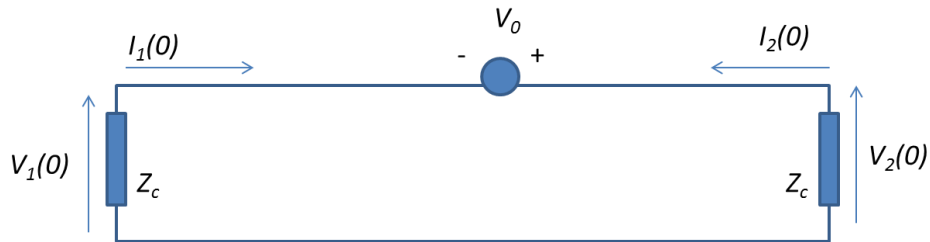


Figure 5 : Equivalent electrical circuit at low frequency for the  $Z_c/Z_c$  configuration

Figure 6 shows a comparison of the result of the current at  $J_1$  of the one-conductor transmission-line presented in Figure 1 in the following source configurations:

- CRIPTE calculation for a Dirac source  $V_0$  localized at the beginning of the transmission-line (legend "Loc Source Left"),
- CRIPTE calculation for a Dirac source  $V_0$  localized in the Middle of the transmission-line (legend "Loc Source Middle"),
- CRIPTE calculation for a total source  $V_0$  distributed along  $\ell$ , (legend "Dist Source"),
- Analytical calculation for the low frequency approximation (legend "BF approx.").

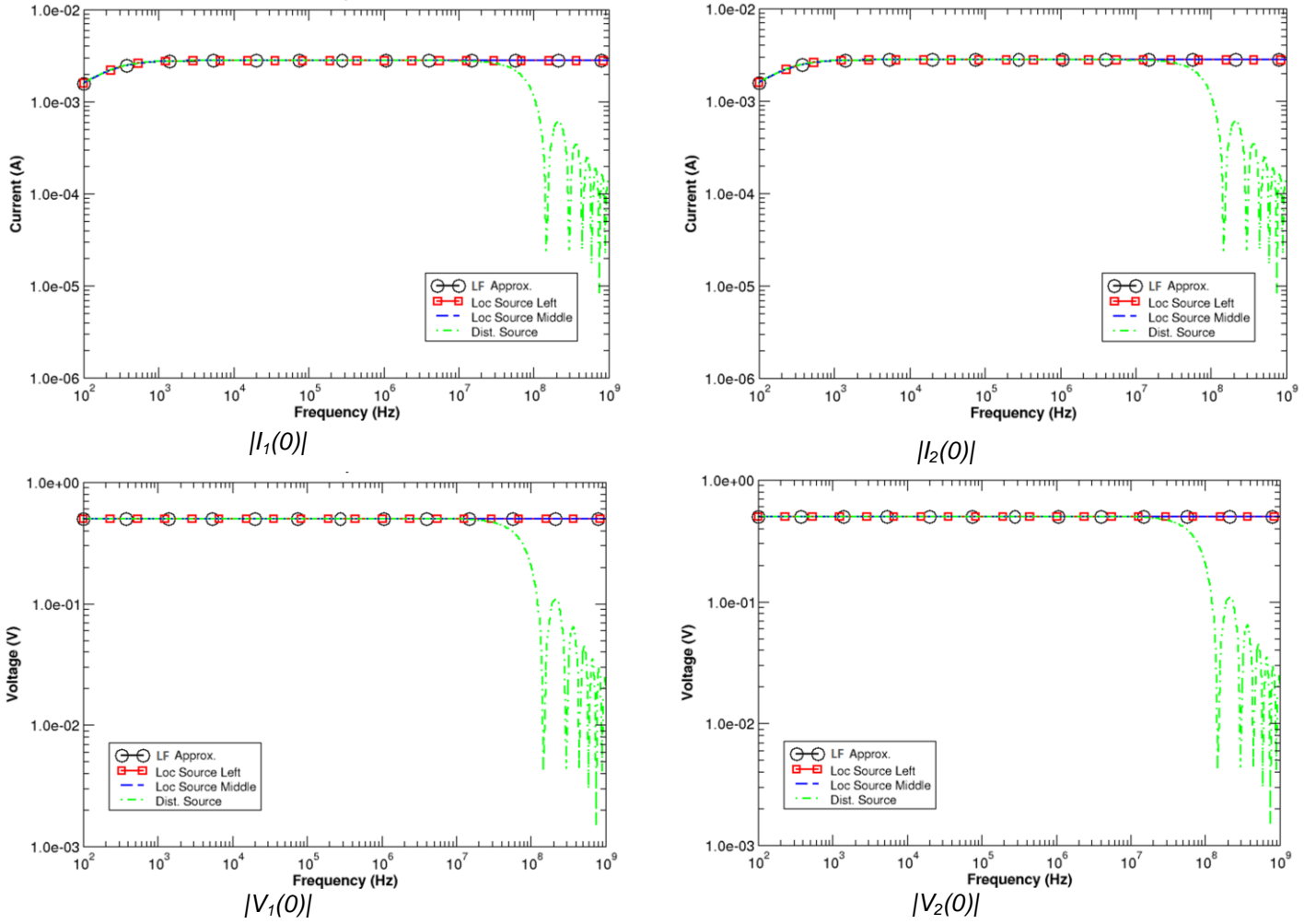


Figure 6 : Comparisons of magnitudes of currents and voltages obtained in  $Z_c/Z_c$  configuration ( $V_0=1V$ )

The following observations can be made:

- At low frequency, the four plots are superposed which demonstrates that at low frequency, the result does not depend on the position of the source (equations).
- At low frequency, voltages are constant as expected in (52) whereas currents are varying with frequency (53) because of the dependence of  $Z_c$  with frequency itself at low frequency

( $Z_c = \sqrt{-j \frac{R}{C\omega} + \frac{L}{C}}$ ). After a cutoff frequency equal to  $f_c = \frac{R}{2\pi L} = 292$  Hz (with the p.u.l.

parameters defined in 2.1,  $Z_c$  becomes constant and equal to  $Z_c = \sqrt{\frac{L}{C}} = 180 \Omega$ .

- Note that, at high frequency, the responses vary in the signal as  $\frac{\sinh(x)}{x}$  (see (37) and (41)). The

flat response of the voltage expected in the resonance region for the localized voltage source is not anymore valid for distributed sources. This results in maxima and minima and the attenuation of the voltage and current responses with frequency.

#### 5.4. Low frequency SC/OC analysis

From (54) we note that the equivalent voltage at the level of the open circuit at  $J_2$  is equal to  $V_0$ , whatever the distribution between  $d_1$  and  $d_2$  which sounds logical from a circuit analysis point of view. However, we note from (55) to (58) that the value of the short-circuit current at the level of  $J_1$  depends on the positions  $d_1$  and  $d_2$ .

From an electrical circuit point of view, this means that only the part of the capacitance located between  $\ell_i$  and the end open circuit contributes to the derivation of the current, the part distributed between the end short-circuit and  $\ell_i$  being somewhat short-circuited (Figure 7).

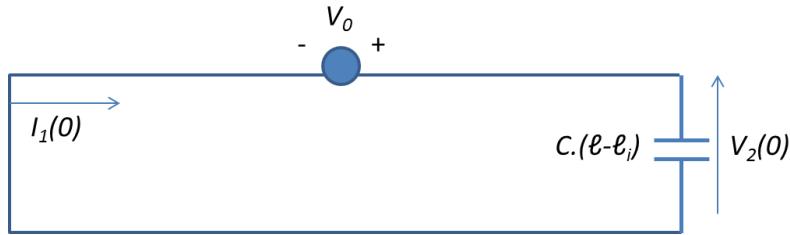


Figure 7 : Equivalent electrical circuit at low frequency for the SC/OC configuration

Figure 8 shows a comparison of the current and voltage calculated by CRIPTE and with analytical formulas for the case of a Dirac source  $V_0 = 1V$  localized at the beginning of the transmission-line presented in Figure 1 (p.u.l; capacitance  $C=18.5$  pF/m).

- CRIPTE calculation for a Dirac source  $V_0 = 1V$  localized at the beginning of the transmission-line ( $\ell_i=0$ ) (legend "Loc Source Left"),
- CRIPTE calculation for a Dirac source  $V_0 = 1V$  localized in the middle of the transmission-line ( $\ell_i=\ell/2$ ) (legend "Loc Source Middle"),
- CRIPTE calculation for a total source  $V_0 = 1V$  uniformly distributed along  $\ell$  (legend "Dist Source"),
- Analytical calculation for the low frequency approximation of a Dirac source  $V_0 = 1V$  localized at the beginning of the transmission-line (legend "BF Loc Source Left").
- Analytical calculation for the low frequency approximation of a Dirac source  $V_0 = 1V$  localized in the middle of the transmission-line and uniformly distributed along  $\ell$  (legend "BF Loc Source Middle & Dist"); indeed, the low frequency approximation gives the same responses (equations (57) and (58)).

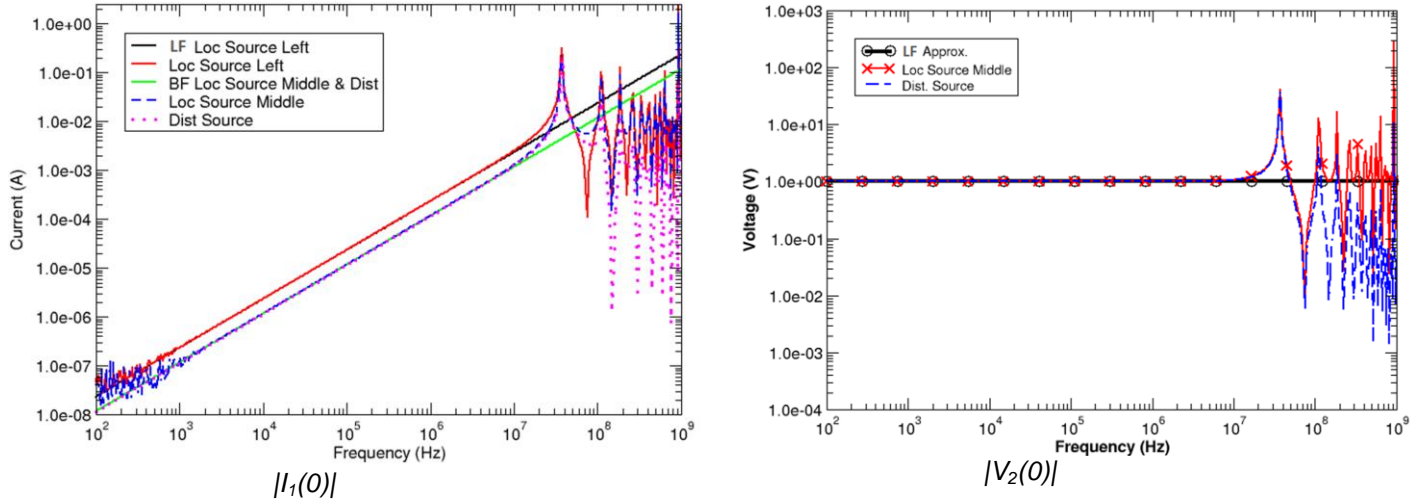


Figure 8 : Comparisons of magnitudes of current  $I_1(0)$  and voltage  $V_2(0)$  obtained in SC/OC configuration ( $V_0=1V$ )

The following observations can be made:

- At low frequency, all current plots vary as  $j\omega$  (equation (55)),
- Some numerical noise is observed in the CRIPTE calculation at low frequency due to the fact that this configuration cannot develop current at DC,
- Unlike the previous SC/SC and  $Z_c/Z_c$  configurations, the current plots are not superposed at low frequency which demonstrates the influence of the position of the source (equations (42) to (45)).
- All voltages are equal at low frequency, whatever the distribution of the source is (equation (54)),
- In the resonance region, all the currents resonate in  $\lambda/2$ , as expected with the denominators of (42). For distributed sources we note a damping for the distributed source configuration that can be explained by the presence of  $\gamma \cdot Z_c = Z$  at the denominator of (45).

## 6. INFLUENCE OF SOURCES DISTRIBUTED ON SEVERAL SEGMENTS

### 6.1. Position of the problem

We consider now a series of  $N$  total constant sources  $V_{0,i}$  distributed on intervals  $[d_i, d_{i+1}]$ . We also consider that the sum of those total sources on the whole length  $\ell$  is equal to  $V_0$ . We write:

$$\sum_{i=1}^N V_{0,i} = V_0 \quad (59)$$

According to (25), assuming:

$$\begin{aligned} d_i &= \ell_i - \Delta \ell_i \\ d_{i+1} &= \ell_i + \Delta \ell_i \\ \ell_i &= (d_i + d_{i+1})/2, \end{aligned} \quad (60)$$

each of those total  $V_{0,i}$  sources may be approximated by  $V_{sd,i}$  Dirac sources centered in  $\ell_i$ . The amplitudes of the Dirac sources are thereby:

$$V_{sd,i} = \frac{V_{0,i}}{2\gamma\Delta\ell_i} (e^{\gamma\Delta\ell_i} - e^{-\gamma\Delta\ell_i}) = \frac{V_{0,i}}{\gamma\Delta\ell_i} \sinh(\gamma\Delta\ell_i) \quad (61)$$

With this new distribution, the superposition theorem allows finding the resulting currents,  $I_1(0)$ ,  $I_2(0)$ , and voltages,  $V_1(0)$ ,  $V_2(0)$ , at both ends of the transmission-line as the sum of the currents and voltages due to each constant voltage source separately,  $I_{1,i}(0)$ ,  $I_{2,i}(0)$ ,  $V_{1,i}(0)$  and  $V_{2,i}(0)$ .

Hereafter, we will take again the three previously studied configurations SC/SC,  $Z_c/Z_c$  and SC/OC and apply this new distribution of current sources and look at their low frequency approximations.

## 6.2. Configuration SC/SC

From (33), we can write:

$$I_1(0) = \sum_{i=1}^N I_{1,i}(0) \xrightarrow{\omega \rightarrow 0} \frac{\sum_{i=1}^N V_{0,i}}{Z\ell} = \frac{V_0}{Z\ell} \quad (62)$$

And we obtain the same low frequency result for  $I_2(0)$ . The result is exactly similar to (51). The low frequency approximation of the currents and voltages can be obtained by taking the integral of the voltage sources.

## 6.3. Configuration $Z_c/Z_c$

From (52) and (53), we can write:

$$V_1(0) = \sum_{i=1}^N V_{1,i}(0) \xrightarrow{\omega \rightarrow 0} -\frac{\sum_{i=1}^N V_{0,i}}{2} = -\frac{V_0}{2} \quad (63)$$

$$I_1(0) = \sum_{i=1}^N I_{1,i}(0) \xrightarrow{\omega \rightarrow 0} \frac{\sum_{i=1}^N V_{0,i}}{2Z_c} = \frac{V_0}{2Z_c} \quad (64)$$

And we obtain the same low frequency result for  $I_2(0)$  and  $V_2(0)$ . The result is exactly similar to (52) and (53) in the case of a unique source segment. The low frequency approximation of the currents and voltages can be obtained by taking the integral of the voltage sources.

## 6.4. Configuration SC/OC

### 6.4.1. General solution

From (54) and (55), we can write:

$$V_2(0) = \sum_{i=1}^N V_{2,i}(0) \xrightarrow{\omega \rightarrow 0} \sum_{i=1}^N V_{0,i} = V_0 \quad (65)$$

$$I_1(0) = \sum_{i=1}^N I_{1,i}(0) \xrightarrow{\omega \rightarrow 0} \sum_{i=1}^N V_{0,i} \frac{\gamma}{Z_c} (\ell - \ell_i) = \frac{\gamma}{Z_c} \left( V_0 \cdot \ell - \sum_{i=1}^N V_{0,i} \cdot \ell_i \right) \quad (66)$$

Introducing the per-unit-length capacitance and still assuming that the per-unit-length conductance is equal to zero, (66) can be written as:

$$I_1(0) = j\omega C \ell \left( V_0 - \sum_{i=1}^N V_{0,i} \frac{\ell_i}{\ell} \right) \quad (67)$$

Equation (65) shows that the voltage at the level of the open-circuit remains equal to the sum of all the distributed generators,  $V_0$ . However, (66) or (67) clearly show that the current at the level of the short-circuit cannot be deduced from  $V_0$  only. More, the value of the current depends on the distribution of the sources on the intervals.

#### 6.4.2. Application

As an illustration, we show three calculations of 2 distributed constant sources,  $V_{0,1}$  and  $V_{0,2}$ , for which the integral is equal to  $V_0 = V_{0,1} + V_{0,2}$  and respectively positioned at  $\ell/4$  and  $3\ell/4$  with  $d_1 = 0$ ,  $d_2 = \ell/2$ ,  $d_3 = \ell$ .

Configuration 1:  $V_{0,1} = 2V_0$  and  $V_{0,2} = -V_0$ :

$$I_1(0) = jC\omega \left( \ell - \frac{\ell}{4} \right) 2V_0 + jC\omega \left( \ell - \frac{3\ell}{4} \right) (-V_0) = jC\omega \left( \frac{3}{2} - \frac{1}{4} \right) \ell V_0 = jC\omega \frac{5}{4} \ell V_0$$

Configuration 2:  $V_{0,1} = -V_0$  and  $V_{0,2} = 2V_0$ :

$$I_1(0) = jC\omega \left( \ell - \frac{\ell}{4} \right) (-V_0) + jC\omega \left( \ell - \frac{3\ell}{4} \right) 2V_0 = jC\omega \left( -\frac{3}{4} + \frac{1}{2} \right) \ell V_0 = -jC\omega \frac{1}{4} \ell V_0$$

Configuration 3:  $V_{0,1} = 1/2 V_0$  and  $V_{0,2} = 1/2 V_0$ :

$$I_1(0) = jC\omega \left( \ell - \frac{\ell}{4} \right) \frac{1}{2} + jC\omega \left( \ell - \frac{3\ell}{4} \right) \frac{1}{2} = jC\omega \left( \frac{3}{8} + \frac{1}{8} \right) \ell = jC\omega \frac{1}{2} \ell$$

### 6.5. Equivalent source solution for low frequency approximation

#### 6.5.1. General solution

As far as low frequency is concerned, the question is now to determine if an equivalent source solution consisting in the application of a unique voltage generator  $V_{eq}$  localized at a given position  $\ell_{eq}$  or distributed between two positions  $d_{1,eq} = \ell_{eq} - \Delta\ell_{eq}$  and  $d_{2,eq} = \ell_{eq} + \Delta\ell_{eq}$  can be found for any of the three loading conditions considered in this paper. We have seen that SC/SC configurations and  $Z_c/Z_c$  configurations did not imply any constraint on the positions of the distributed voltage generators  $V_{0,i}$  provided that the total source remained  $V_0$ . The main constraint is for the SC/OC configuration for which the solution depends on the positions of the  $V_{0,i}$ . Nevertheless, in the three load configurations, the current and voltage solutions at low frequency do not depend on  $\Delta\ell_i$ ; its value can thereby be chosen in order to facilitate the use of the model. The research on the equivalent source must thereby focus on this SC/OC configuration and should directly be valid for the two other configurations.

The equivalence with a localized voltage source can be made by identification of equations (55) and (67) on  $I_1(0)$ . We have:

$$I_1(0) \xrightarrow{\omega \rightarrow 0} jC\omega(\ell - \ell_{eq})V_{eq} = j\omega C\ell \left( V_0 - \sum_{i=1}^N V_{0,i} \cdot \frac{\ell_i}{\ell} \right) \quad (68)$$

Where  $V_{eq}$  represents the equivalent voltage and  $\ell_{eq}$  the equivalent position of this source. Because of the condition (54) on  $V_2(0)$ , we have necessarily:

$$V_{eq} = \sum_{i=1}^N V_{0,i} = V_0 \quad (69)$$

Therefore, we can rewrite (68) as:

$$I_1(0) \xrightarrow{\omega \rightarrow 0} jC\omega(\ell - \ell_{eq})V_0 = j\omega CV_0 \left( \ell - \sum_{i=1}^N \frac{V_{0,i} \ell_i}{V_0} \right) \quad (70)$$

From which, by identification, we have:

$$\ell_{eq} = \sum_{i=1}^N \frac{V_{0,i} \ell_i}{V_0} \quad (71)$$

Consequently, the  $\ell_{eq}$  equivalent position of the Dirac source depends on the distributed voltages and their position. As far as the user wants to use a distributed source instead of a localized source, a value of  $\Delta\ell_{eq}$  must be chosen. We propose to choose  $\Delta\ell_{eq} = \ell/2$ . Note however that the equivalent interval limits,  $d_{1,eq}$  and  $d_{2,eq}$ , can be outside the real boundary limits of the transmission-line ( $[0, \ell]$ ).

Note that the results of this paper also cover a load configuration for which both ends of the transmission-line are in open circuit. Indeed, in this case, the BLT resolution directly gives  $I_1(0)$  and  $I_2(0)$  equal to 0, whatever the source is. In addition, by resolution of (8) with  $S_1 = S_2 = 1$ , the reader may verify that the wideband result is dual of the SC/SC configuration and that the low frequency voltages vary as  $V_1(0) = V_2(0) = V_0$ .

### 6.5.2. Application

As a first application, we choose the same voltage source distribution configuration as in the application described in section 6.4.2 on the one-conductor transmission-line presented in Figure 1. Here after we indicate the equivalent values of  $\ell_{eq}$  and introduced them in equation (55) low frequency formulation. We find again the three  $j\omega$  variations found previously in 6.4.2.

**Configuration 1:**  $V_{0,1} = 2V_0$  and  $V_{0,2} = -V_0$ :

$$\ell_{eq} = \frac{2V_0 \cdot \frac{\ell}{4} - V_0 \cdot \frac{3\ell}{4}}{V_0} = -\frac{\ell}{4} \quad \text{and} \quad I_1(0) = jC\omega V_0 \cdot (\ell - \ell_{eq}) = jC\omega \frac{5}{4} \ell V_0$$

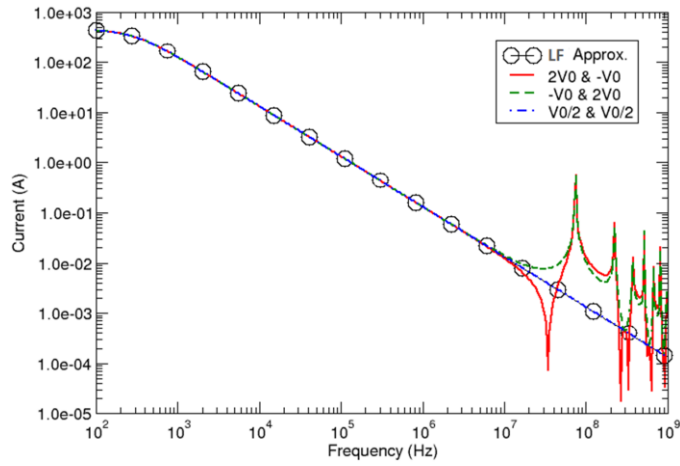
**Configuration 2:**  $V_{0,1} = -V_0$  and  $V_{0,2} = 2V_0$ :

$$\ell_{eq} = \frac{-V_0 \cdot \frac{\ell}{4} + 2V_0 \cdot \frac{3\ell}{4}}{V_0} = \frac{5\ell}{4} \quad \text{and} \quad I_1(0) = jC\omega V_0 \cdot (\ell - \ell_{eq}) = -jC\omega \frac{1}{4} \ell V_0$$

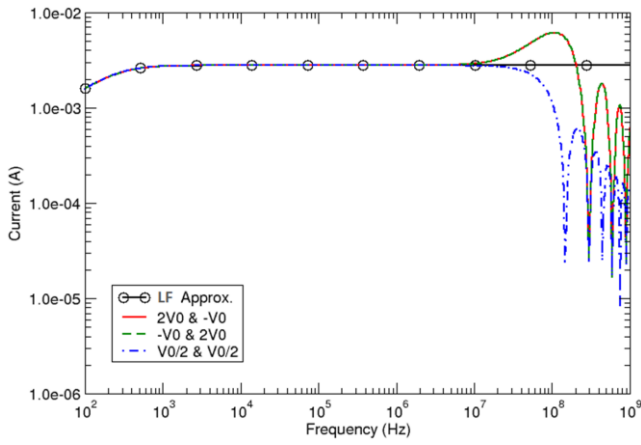
**Configuration 3:**  $V_{0,1} = 1/2 V_0$  and  $V_{0,2} = 1/2 V_0$ , (equivalent to totally distributed sources)

$$\ell_{eq} = \frac{\frac{V_0}{2} \cdot \frac{\ell}{4} + \frac{V_0}{2} \cdot \frac{3\ell}{4}}{V_0} = \frac{\ell}{2} \quad \text{and} \quad I_1(0) = jC\omega V_0 \cdot (\ell - \ell_{eq}) = jC\omega \frac{1}{2} \ell V_0$$

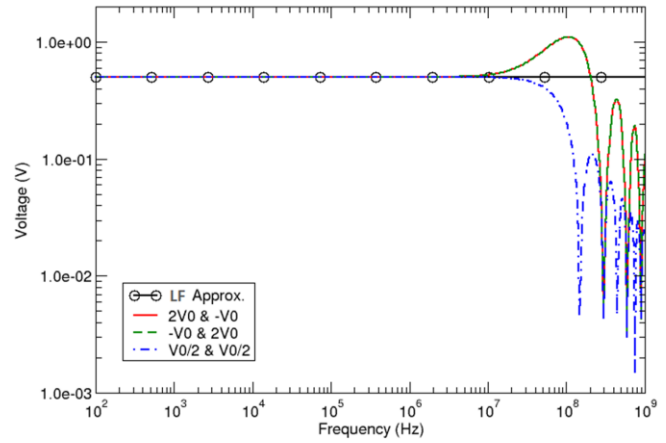
Figure 9 shows the CRIPTE  $I_1(0)$  and  $V_2(0)$  calculations made in the SC/SC,  $Z_c/Z_c$  and SC/OC load configurations when applying the equivalent source as defined in (69) and (71) in the 3 configurations of distributed sources (respectively legends " $2V_0$  &  $-V_0$ ", " $-V_0$  &  $2V_0$ " and " $V_0/2$  &  $V_0/2$ "). Results at low frequency are compared to the low frequency approximations using the model of the unique equivalent source, equally distributed between  $d_{1,eq}$  and  $d_{2,eq}$  (legend "BF Approx."). The results confirm the previous results obtained in the applications in paragraph 6.4 as well as the use of the equivalent source model. On the one hand, we see that voltages  $V_2(0)$  and  $I_1(0)$  currents in  $Z_c/Z_c$  and SC/OC configurations are obtained either from the integral field distributions (voltage in SC/SC configuration is of course zero) distributed on the whole length of the line, either from the equivalent source. On the other hand, even if  $I_1(0)$  currents in SC/OC configuration depend on the source distribution, for the low frequency approximation of the application of the unique equivalent source provides the correct result.



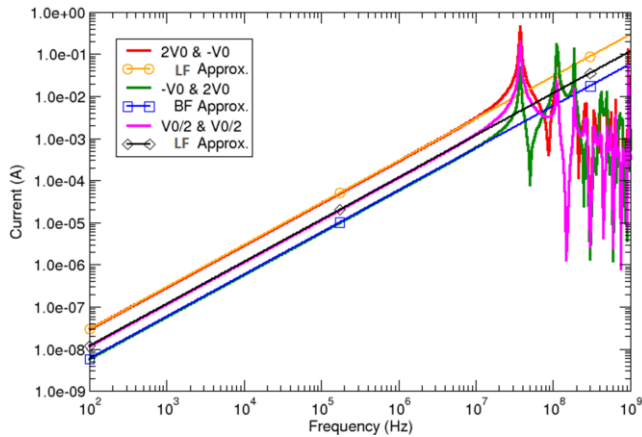
$|I_1(0)|$  in SC/SC configuration



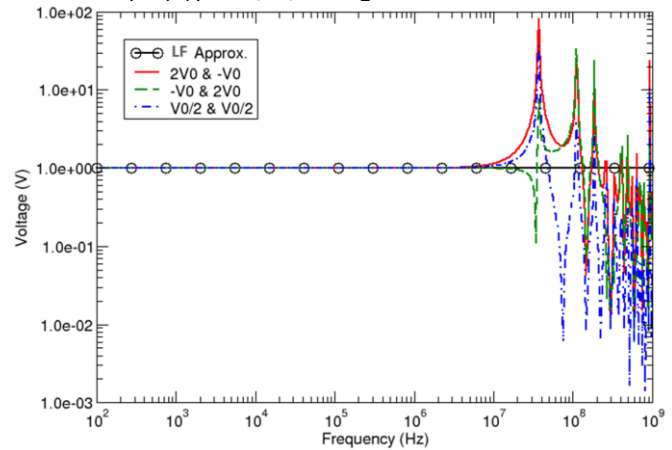
$|I_1(0)|$  in  $Z_c/Z_c$  configuration



$|V_2(0)|$  in  $Z_c/Z_c$  configuration



$|I_1(0)|$  in SC/OC configuration



$|V_2(0)|$  in SC/OC configuration

Figure 9 : Comparisons of magnitudes of current  $I_1(0)$  and voltage  $V_2(0)$  in SC/SC,  $Z_c/Z_c$  and SC/OC configurations, applying the equivalent source model for three distributions of 2 sources giving the same total voltage ( $V_0=1V$ ) along the transmission-line.

## 7. CONCLUSION

In the past 10 years, theoretical research on transmission-lines has mainly addressed the problem of the extension of the theory toward high frequencies, with the willingness to maintain the efficiency and simplicity of the technique while taking into account higher modes beyond the TEM mode [11]. However recent industry projects of full composite aircraft and their consequence in terms of protection against lightning indirect effects and optimization of current return networks have renewed the interest for the application of transmission-line models at low frequency [12]. This paper concentrates on this low frequency aspect for the application of Field-to-Transmission-Line and the capability of the BLT equation formulation to describe electrical circuit models. Indeed this paper also gives the opportunity to show that the BLT solution covers the electrical circuit solution at low frequency, which is not so obvious since the BLT equation is first of all formulated in terms of “waves” and not explicitly in terms of “voltages and currents” which would rather indicate the use of this equation for situations in which propagation is relevant. Nevertheless, the generalization of this property when the per-unit-length conductance of the transmission-line is not equal to zero has not been shown in this paper and remains to be done.

In this document, we have studied in which conditions we could consider that the integral of voltage source terms could be sufficient in order to obtain low frequency solutions of currents on transmission-lines illuminated by incident EM fields. For this, we have analytically studied the case of a single-conductor transmission-line loaded at its ends. We have shown that this approach was sufficient for low-impedance loading conditions at the end of wires and this condition could be extended to load conditions up to matching conditions.

Nevertheless, this integration of voltage sources cannot be extended anymore to high-impedance loading conditions. The study of short-circuit/open circuit configurations shows that the result depends on the location where the source is applied on the transmission-line and thereby on the way the distribution of voltage sources is made on intervals along the transmission-line.

Consequently, the fact that some difference may be observed between “full-3D-sources” and “integrated-sources” approaches when integrating distributed source terms in segments along cable paths is not an error of the BLT solution implementation. The reason of this difference comes from the application of the MTL model. The most exact solution remains the “full-3D-sources” solution which, by the way, remains an approximated solution due to the discretization approximation made in the 3D computer code. However, it is important to realize that in such low-impedance conditions, the relevant observable is not the current but the voltage and the fact of making an error on low-level currents would be indeed more acceptable than making an error on high level currents!

However, in terms of applications at aircraft level, investigation of the values of loads at the end of the wires is not practically possible, especially if loads vary with frequency, being aware of the difference that can be observed for low amplitude currents is important. The equivalent source model developed at the end of this paper is based on the determination of an equivalent center position. This equivalent position is determined from an integration of the voltage source terms on intervals weighed by the length of those intervals. This leads to a simplified model of low-frequency equivalent source, universal in the sense that it does not depend on the value of loads under consideration. Note that the equivalence is only mathematical since the boundaries of application of the source are generally outside of the boundaries of the transmission-line.

Next steps of the research on this topic will consist in implementing this technique in computer modelling environments such as CRIPTE and in applying it on complex test-cases such as at aircraft level.

## 8. REFERENCES

- [1] C. E. Baum, T. K. Liù, F. M. Tesche, "On the Analysis of General Multiconductor Transmission-Line Networks, *Interaction Notes*", Note 350, November 1978
- [2] J.P. Parmantier, X. Ferrières, S. Bertuol, C. E. Baum : "Various Ways to Think of the Resolution of the BLT Equation with an LU Technique". *Interaction Notes*. Note 535. January 1998.
- [3] FAA Advisory Circular "Certification of Electrical Wiring Interconnection Systems on Transport Category Airplanes", AC No. 25.1701-1
- [4] F.M. Tesche, M.V. Ianoz, T. Karlsson, "EMC Analysis Methods and Computational Models", John Wiley & Sons, pp.247-266. 1997.
- [5] L. Paletta, J-P. Parmantier, F. Issac, P. Dumas, J.-C. Alliot, "Susceptibility analysis of wiring in a complex system combining a 3-D solver and a transmission-line network simulation", *IEEE Trans. on EMC*, Vol. 44, No. 2, May 2002, pp. 309-317.
- [6] X. Ferrières, J-P. Parmantier, S. Bertuol, A. Ruddle, "Application of Hybrid Finite Difference / Finite Volume to Solve an Automotive problem", *IEEE Trans. on EMC*, vol 46, n°4, pp. 624, 634, November 2004
- [7] J-P. Parmantier, M. Ridel, S. Bertuol, I. Junqua, C. Giraudon, C. Girard, F. Terrade, J-P. Moreau, "Modelling of HIRF coupling on complex cable architectures," in *Electromagnetics in Advanced Applications (ICEAA)*, 2011, pp. 219-222. September 2011.
- [8] F Rachidi, "Formulation of the field-to-transmission-line coupling equations in terms of magnetic excitation field", *IEEE Transactions on EMC*, 1993
- [9] J.P. Parmantier, "The test-wiring method". *Interaction Notes*. Note 553. October 1998.
- [10] J. P. Parmantier, S. Bertuol, and I. Junqua, "CRIPTE : Code de réseaux de lignes de transmission multiconducteur - User's guide – Version 5.1" ONERA/DEMR/T-N119/10 - CRIPTE 5.1 2010.
- [11] F. Rachidi, S. Tkachenko: "Electromagnetic Field Interaction with Transmission-lines", *Advances in Electrical Engineering and Electromagnetics #5*, 2008
- [12] I. Junqua, J-P. Parmantier, D. Prost: "Modelling Common Mode Impedances for Lightning Indirect Effects on Multiconductor Cables into Composite Aircraft Equipped with Current Return Networks", *Proceeding of ICOLSE 2015 Conference*, Toulouse, September 2015
- [13] G. Andrieu, L. Koné, F. Bocquet, B. Démoulin, J-P. Parmantier, "Multiconductor Reduction Technique for Modeling Common Mode Current on Cable Bundles at High Frequency for Automotive Applications". *IEEE Trans; on EM Compatibility*, vol 50, n°1, February 2008